

Understanding the processes associated with the intraseasonal sea surface temperature variability in the Northern Indian Ocean during boreal summer

A. Jayakumar, C.Gnanaseelan, J.Vialard

- Estimate the relationship between the observed intraseasonal SST and the observed satellite flux in the SST variance maxima regions in the North Indian Ocean (NIO) during boreal summer
- Quantify the respective role of different processes associated with intraseasonal SST signature (30-90 day and 10-30 day band) using Ocean General Circulation Model(OGCM) sensitivity experiments.

Introduction:

The predictability of the Indian summer monsoon would depend on relative contribution of Intraseasonal Oscillations(ISOs) to the seasonal mean in compared to the externally forced component. These atmospheric ISOs classified into a broadband spectrum of scale between 10 and 90 days with two preferred bands of periods of 30-90 day and 10-30 day time scale. Former bandwidth generally named as Madden-Julian Oscillation (MJO) [e.g., Madden and Julian, 1971] having distinct character in summer from the boreal winter and later as submonthly where westward moving convectively coupled waves dominates.(Wheeler and Kiladis, 1999). The local coupled Indian Ocean air-sea interaction basically governs the structure and the phase propagation of aforementioned ISOs. Tropical ocean affects the atmosphere via sea surface temperature (SST) through which mainly control the local coupled processes, hence investigating processes associated with the intraseasonal SST is key to understand. The different basin of the Indian Ocean for the summer season over NIO responds differently.

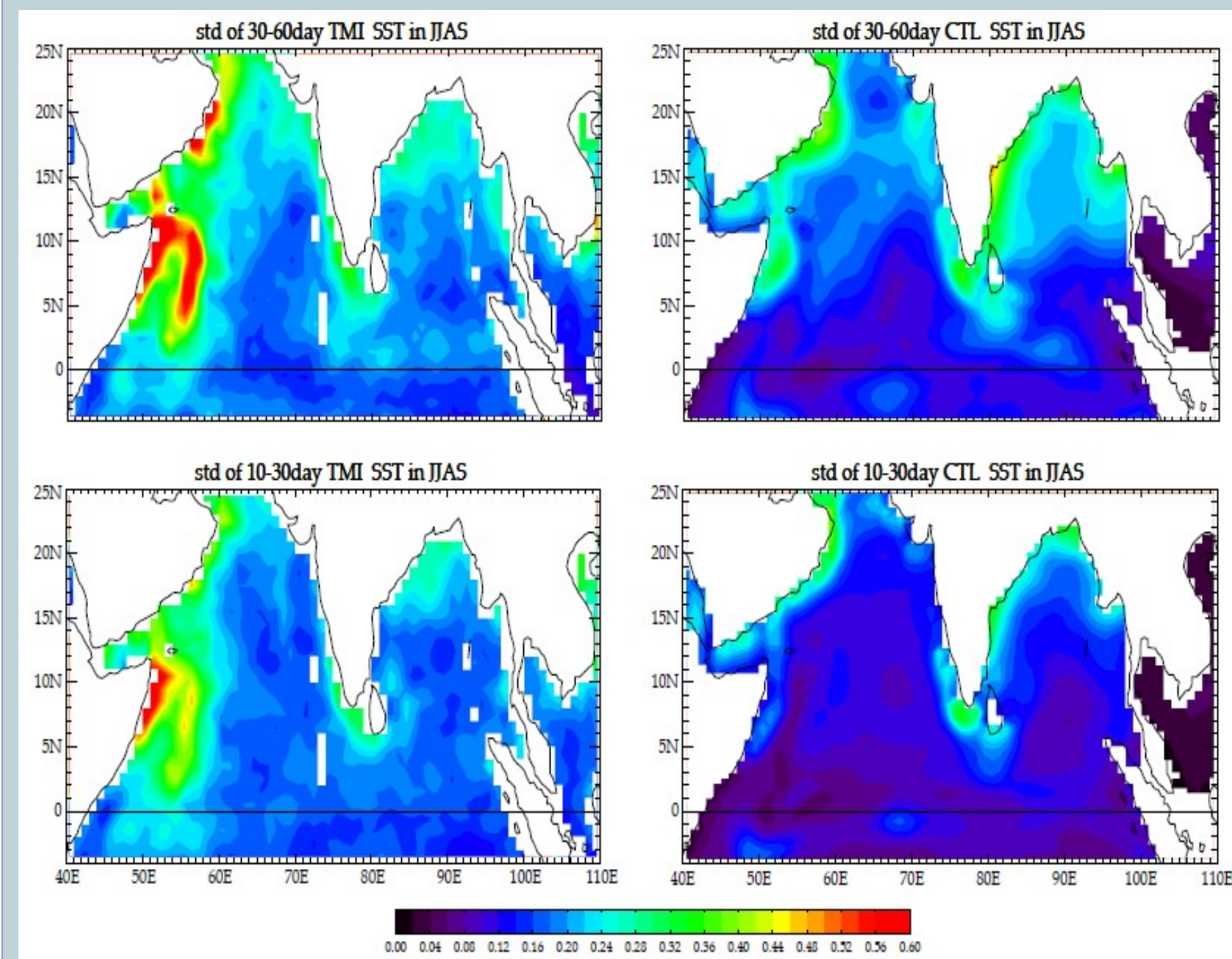


Fig. 1: (left panels) SD of band pass TMI (30-60 days) and (10-30 days) SSTA (right panels) SD of band pass CTL(30-60 days) and (10-30 days) SSTA for JJAS

Data and Methodology and Model:

(a. Datasets used to get idea of the oceanic structure of NIO): Mixed layer depth (MLD) climatology from de Boyer et al. (2004) and depth of the 20°C isotherm derived from the World Ocean Atlas 2005 (WOA05). The barrier layer depth (BLT) climatology also derived from de Boyer et al. (2004) where they defined as the depth difference of the isothermal layer depth (0.2°C drop of temperature from surface) to the MLD where the same criteria is used for estimating the model based BLT. **(b. Datasets to estimate ISOs surface signals):** We have used 0.25° x 0.25° fields of 3-day mean SST measured by the Microwave Imager on-board the TRMM satellite (TMI). The NOAA interpolated 2.5° x 2.5° outgoing long wave radiation (OLR) is used as a proxy for convection in this study. We used gridded fields of wind parameters as retrieved from the NASA SeaWinds scatterometer, onboard QuikSCAT over 0.5°x0.5° resolution. We merged ERA-40 wind with QuikSCAT for the period prior to January 2000. To estimate the air-sea flux associated with the ISOs we used latest version of global ocean-surface heat flux products developed by the Objectively Analyzed air-sea Heat Fluxes (OAFlux) project over 1.0°x1.0° resolution (Yu et al., 2008). All these observed satellite surface flux products are analysed for the period of 1998-2007, so that final daily data for each product was averaged to a common one-degree daily grid. **(c. Filtering Methods):** To isolate the signal associated with the summer ISOs, we have used band-pass filtering (Duchon, 1979) of daily anomalies with respect to the mean seasonal cycle with a weighting function of 121 days. **(d. Model Experiments):** The OGCM used in the present study is the latest version of Geophysical Fluid Dynamics Laboratory (GFDL) Modular Ocean Model (MOM4) and is set up for the region between 40°S-25°N and 30°E-120°E and has 30 vertical levels. The sensitivity experiments, have been set up by symmetrically retain the full spectrum of heat flux forcing as CTL for the flux computation while, the boundary conditions for the momentum equation have been changed. The details of the experiments given Table 1. and its significance are discussed detailed in Jayakumar et al, 2010.

Results:

1. Background oceanic structure of the NIO for summer intraseasonal SST variability:- The mixed layer in the Arabian Sea (maximum of ~80m) is deeper compared to the Bay of Bengal (maximum being ~40m) basin due to the turbulent vertical mixing associated with strong south-westerly monsoon wind over the Arabian Sea and strong stratification in the BoB due to the river discharge and the rainfall. This shallow mixed layer prevailed in the BoB has strong association with the coherent evolution of intraseasonal SST with the net heat flux perturbation. The fresh water discharge is favourable for the formation of barrier layer in the BoB (maximum thickness is 40m) by limiting the mixed layer by haline stratification thereby strengthening the SST variance by forced surface fluxes.

Acknowledgements: Authors acknowledge Director, IITM for his encouragement and CSIR for supporting the work, organizers of Workshop on Modelling Monsoon Intraseasonal Variability for travel and other financial support.

Name	Forcing	Description
CTL	Full forcing	Main Solution
NO_ISO_FLUX	Low-passed filtered shortwave and net heat fluxes.	Isolate intraseasonal flux variability
NO_ISO_STRESS	Low-passed filtered wind stress	Isolate intraseasonal wind stress variability
NO_ISO	Low passed filtered shortwave and net heat fluxes, Low passed filtered wind stress	Isolate Internal variability
NO_ISO_SW	Low passed filtered shortwave flux	Isolate intraseasonal shortwave variability

Table 1:- List of Experiments used in this study

Figure 1 show the regions of maximum intraseasonal SST variability (Standard deviation (SD) of 30-60 day and 10-30 day filtered TMI(left panels) and control experiment (CTL, see Table 1) (right panels) SST during summer. It indicate the regions of maximum intraseasonal variability in the NIO during summer, these regions coincide with the regions of strong wind perturbation and convection as in Duvel and Vialard (2007). Though the model captured the spatial pattern of the intraseasonal variability and are comparable with the observations, in general the strength of the simulated intraseasonal SST variability is weaker than the observation, hence can be used to assess the importance of various processes associated with this variability.

2. Intraseasonal air-sea interaction associated with summer ISOs in NIO

Figure 2(a) shows the regression relation between the intraseasonal SST (30-90 day band) and the intraseasonal OLR and wind speed. The asymmetry in this curve infers the difference in the ocean response to the cloud condition (dry and wet phases of ISOs). The typical time scale of perturbations is 40-50 days. Regressed SST in the MJO time scale shows the peak amplitude in the positive phase and is around ~0.45°C in the OMAN region followed by ~0.4°C in BoB, ~0.25°C in STI and ~0.25°C in WAS. But for OLR, the maximum amplitude (20 Wm⁻²) is seen in the BoB with SST lagging OLR by ~10 days. This highlights the role of surface insolation in driving intraseasonal SST in the BoB. The spatial structure of the regressed surface fields (OLR and wind fields) with reference to the BoB intraseasonal SST resembles the observed canonical northward-propagating ISO events (Figure 3). OLR can be used as a sensitive indicator and proxy for large-scale convection and precipitation over the NIO region. Similar horizontal picture of the regressed surface fields based on the other basins (OMAN and STI) except WAS (Figure 3b).

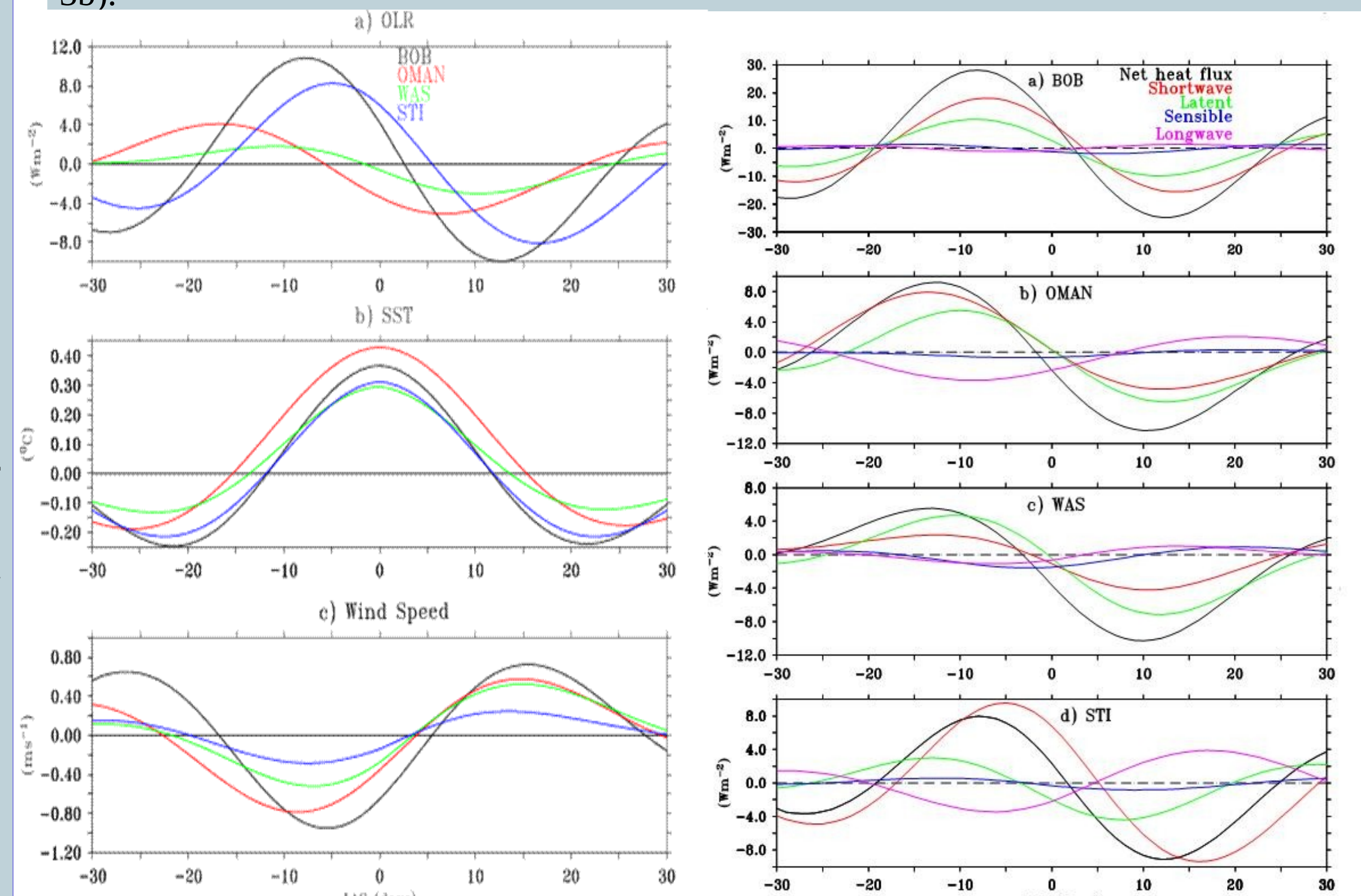


Fig. 2a:- Intraseasonal (30-90day) SST in the NBoB (black), OMAN (red), WAS(green), STI(blue) region regressed to 30-90 day band-passed a) outgoing long wave (OLR) b) SST c) Wind speed in the respective regions for JJAS.

Fig. 2b:- Intraseasonal (30-90day) net heat flux (black) perturbation and its components: latent heat(green), shortwave(red), sensible(blue) and longwave(pink) regressed to the intraseasonal SST(30-90 day) for a) BOB b) OMAN c) WAS d) SWB region for JJAS period.

The flux components are regressed on the intraseasonal SST in the selected regions (Figure 2b). The peak-to-peak amplitude of net heat flux perturbation is 60 Wm⁻² in the NBoB and in phase relation with dominant contributors such as short wave and latent heat flux and a negligible amount from long wave and sensible heat flux. Around two-third of the net heat flux fluctuation is provided by shortwave flux forced by the cloud fluctuation and remaining one-third is contributed by the latent heat flux forced by the intraseasonal winds. The net heat flux contribution in the OMAN region is dominated by the latent heat flux and short wave radiation (the latent heat dominating the net heat flux in the active phase) and the long wave radiation contributes negatively to the net heat flux. Over the WAS, the latent heat flux primarily drives the SST variability and is dominant in both active and suppressed phase of ISO. This may be due to the perturbations in the surface winds associated with the LLJ variability. In contrast to the other regions, STI variability is characterized by out of phase flux components.

Submonthly SST variability is weaker than that of MJO scale, whereas the heat flux and momentum flux are comparable to those of MJO. Hence in the case of submonthly, the intensity is lessened by the short period of atmospheric forcing. SST in the sub-monthly scale shows peak amplitude of about 0.6°C in BoB and STI, whereas it is about 0.4 °C in WAS and 0.3 °C in OMAN (Figure not shown). Submonthly SST in the BoB has stronger amplitude than OMAN, contrary to the MJO scale SST response. The net heat flux and its components in the BoB are in phase and the magnitudes are comparable with the MJO scale. Similar in phase relation can be seen in the WAS, except that the long wave flux and sensible flux contribute negatively to the net heat flux. In the OMAN region, the latent heat flux is contributing more to the net heat flux in the warming phase. There is asymmetry in the flux perturbation especially in the latent heat flux. In STI, sub-monthly flux (net heat flux) components are higher (more than double the magnitude) in amplitude compared to the MJO scale forcing. There is no significant influence by longwave flux in this scale whereas in the MJO scale it has reduced the impact of short wave flux significantly.

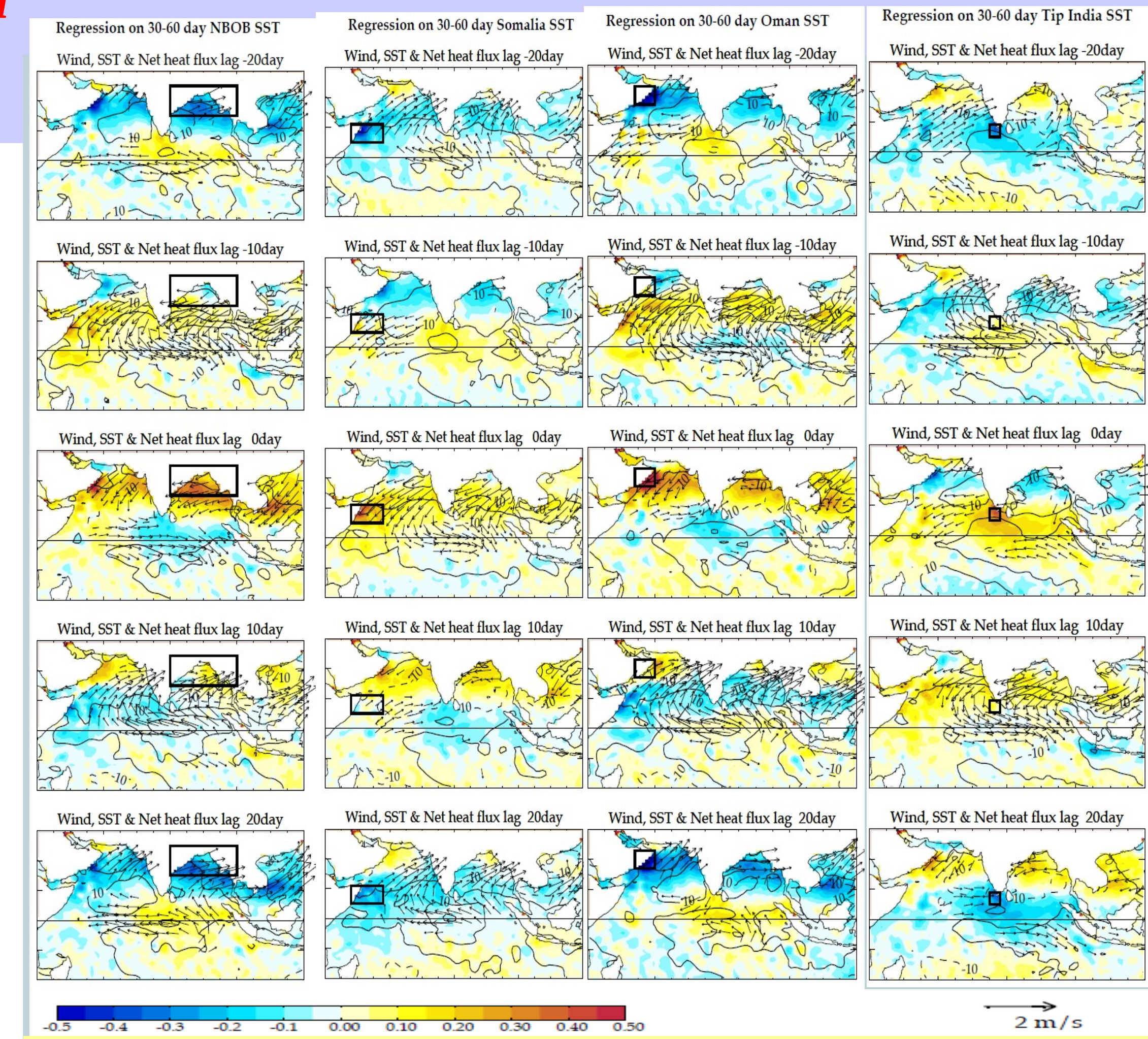


Fig. 3: Regression on (30-60day) NBoB, WAS, OMAN, STI SST with 30-60 day Wind (vector), SST(shaded) and Net heat flux(contour)

The lag regressions (Figure 3) show that the NBoB and OMAN upwelling and STI (smaller amplitude) are strongly tied to the active-break cycle whereas WAS(Somalia upwelling) seems more independent mostly based on the Low level Jet intensity and internal variability influence (Table 2). The SST response follows the northward movement of the active phase (STI first, then Somalia, then NBoB and OMAN shortly after that. In 30-60 day mode even though the surface flux forcing is higher in the BoB, the peak amplitude in SST is observed in the AS basin (OMAN). This made us to go for specifically designed sensitivity experiments to quantify the processes associated with the intraseasonal SST.

3. Processes analysis of the intraseasonal SST signature over NIO

	BoB	OMAN	WAS	STI
All processes (CTL)	1.0	1.0	1.0	1.0
Internal Variability	0.14	0.43	0.49	0.11
Residual	-0.07	0.01	0.01	-0.01
Wind Stress	0.16	0.41	0.32	0.77
Heat Flux	0.77	0.15	0.18	0.16
Shortwave Flux	0.58*	0.12*	0.11*	0.28*

Table 2:- The regression coefficient of the 30-90 day SST variability averaged over the NIO selected regions associated with each process to total 30-90 day variability in the CTL experiment. Note that by construction, the sum of the contribution of internal variability, residual, wind stress and heat flux regression coefficients is equal to 1 (i.e. those can be seen as estimates of the % of variability explained by a certain process).

Summary:

During summer, the northern Indian Ocean exhibits significant atmospheric intraseasonal variability in both the 30-60 day (active and break phases of the monsoon) and 10-30 day (quasi bi-weekly oscillation) bands. Here, we investigate mechanisms of the Sea Surface Temperature (SST) signature in these two frequency bands. To that end, we use 10 years of microwave-derived SST, gridded outgoing long wave radiation (OLR), QuikScat wind and Objectively Analyzed air-sea Heat Fluxes (OAFlux) and several Ocean General Circulation Model (OGCM) sensitivity experiments.

Although surface heat flux perturbations have roughly the same amplitude for the 10-30 day and 30-60 day variability, the SST signature in the 30-60 day band is considerably larger, consistent with the reddening of the spectrum expected from oceanic integration of the atmospheric forcing. There is a significant SST signature in the Arabian Sea (in the Somalia, Oman, and south-western coast of India upwelling regions) in the 30-60 band in addition to the previously-reported SST intraseasonal variability in the Bay of Bengal (BOB). The SST variations in the BOB, Oman upwelling and south-western coast of India regions seem to be tied with active and break phases of the southwest monsoon, while the Somalia upwelling variability seems to be more independent and locally driven by the low-level monsoon jet intensity. The SST signature in the 30-60 day band is larger in the Arabian Sea, whereas air-sea flux perturbations tend to be larger in the Bay of Bengal, suggesting a stronger influence of oceanic processes in the Arabian Sea. Sensitivity experiments with an OGCM suggest that SST intraseasonal variability is largely driven by intraseasonal air-sea flux perturbations in the Bay of Bengal, in agreement with previous studies. On the other hand, SST signature of the 10-30 and 30-60 day variability seem to be largely associated with wind stress perturbations in the Arabian Sea, with a possible significant contribution from internal instabilities in the Oman and Somalia upwelling regions.

References:

- JAYAKUMARA, VIALARD J., M.LENGAIGNE, GNANASEELAN C., McCREARY J.P. and PRAVEEN KUMAR, (2010) *Climate Dynamics*, (Submitted).
- DUCHON, C. E. (1979), *J. Appl. Meteorol.*, 18, 1016–1022.
- DUVEL and VIALARD (2007), *Journal of Climate*, 20, 3056-3082.
- MADDEN, R. A and P. R. JULIAN (1971) *J. Atmos. Sci.*, 28, 702–708, doi:10.1175/1520-0469(1971)
- WHEELER, M and G. N. KILADIS, (1999) *J. Atmos. Sci.*, 56, 374 – 399, doi:10.1175/1520-0469(1999)